

AD A 030876

AFML-TR-76-94

12

ELASTIC RESPONSE OF ROSETTE CYLINDERS UNDER AXISYMMETRIC LOADING

*MECHANICS & SURFACE INTERACTIONS BRANCH
NONMETALLIC MATERIALS DIVISION*

JULY 1976

TECHNICAL REPORT AFML-TR-76-94
INTERIM REPORT FOR PERIOD OCTOBER 1975 - MARCH 1976

Approved for public release; distribution unlimited

DEC
OCT 19 1976
RECEIVED
D

AIR FORCE MATERIALS LABORATORY
AIR FORCE WRIGHT AERONAUTICAL LABORATORIES
AIR FORCE SYSTEMS COMMAND
WRIGHT-PATTERSON AIR FORCE BASE, OHIO 45433

NOTICE


When Government drawings, specifications, or other data are used for any purpose other than in connection with a definitely related Government procurement operation, the United States Government thereby incurs no responsibility nor any obligation whatsoever; and the fact that the Government may have formulated, furnished, or in any way supplied the said drawings, specifications, or other data, is not to be regarded by implication or otherwise as in any manner licensing the holder or any other person or corporation, or conveying any rights or permission to manufacture, use, or sell any patented invention that may in any way be related thereto.

This report has been reviewed by the Information Office (IO) and is releasable to the National Technical Information Service (NTIS). At NTIS, it will be available to the general public, including foreign nations.

This technical report has been reviewed and is approved for publication.


N. J. PAGANO
Project Engineer

FOR THE DIRECTOR


S. W. TSAI, Chief
Mechanics & Surface Interactions Branch
Nonmetallic Materials Division

Copies of this report should not be returned unless return is required by security considerations, contractual obligations, or notice on a specific document.

UNCLASSIFIED

SECURITY CLASSIFICATION OF THIS PAGE (When Data Entered)

REPORT DOCUMENTATION PAGE		READ INSTRUCTIONS BEFORE COMPLETING FORM
1. REPORT NUMBER AFML-TR-76-94	2. GOVT ACCESSION NO.	3. RECIPIENT'S CATALOG NUMBER
4. TITLE (and Subtitle) ELASTIC RESPONSE OF ROSETTE CYLINDERS UNDER AXISYMMETRIC LOADING.	5. DATE OF REPORT & PERIOD COVERED Interim rept. Oct 1975 - Mar 1976	
7. AUTHOR(s) N. J. Pagano	8. CONTRACT OR GRANT NUMBER(s) In-house	
9. PERFORMING ORGANIZATION NAME AND ADDRESS Air Force Materials Laboratory (AFML/MBM) Air Force Systems Command Wright-Patterson AFB, OH 45433	10. PROGRAM ELEMENT, PROJECT, TASK AREA & WORK UNIT NUMBERS 22790102	
11. CONTROLLING OFFICE NAME AND ADDRESS Air Force Materials Laboratory (AFML/MBM) Air Force Wright Aeronautical Laboratories Wright-Patterson AFB, OH 45433	12. REPORT DATE July 1976	
14. MONITORING AGENCY NAME & ADDRESS (if different from Controlling Office) 1237f	13. NUMBER OF PAGES 37	
15. SECURITY CLASS. (of this report) Unclassified		15a. DECLASSIFICATION/DOWNGRADING SCHEDULE
16. DISTRIBUTION STATEMENT (of this Report) Approved for public release; distribution unlimited. 16 AF-2279 17 227901		
17. DISTRIBUTION STATEMENT (of the abstract entered in Block 20, if different from Report)		
18. SUPPLEMENTARY NOTES		
19. KEY WORDS (Continue on reverse side if necessary and identify by block number) Rosette Cylinders Composite Material Heterogeneous Elasticity Carbon/carbon Materials Rosette Characterization		
20. ABSTRACT (Continue on reverse side if necessary and identify by block number) The problem of the elastic response of a rosette cylinder, i.e., a cylindrical body formed by reinforced composite layers wrapped along spiral trajectories, is formulated and solved through the application of the theory of heterogeneous elasticity. It is shown that 21 elastic coefficients, which in general, are functions of position in the medium, enter the elastic constitutive equations. Certain geometric preliminaries and tensor transformation laws establish the relation between these coefficients and the orthotropic moduli of the basic sheet material. It is also demonstrated that problems involving axisymmetric		

DD FORM 1 JAN 73 1473

EDITION OF 1 NOV 65 IS OBSOLETE

UNCLASSIFIED

SECURITY CLASSIFICATION OF THIS PAGE (When Data Entered)

012320 4E

UNCLASSIFIED

SECURITY CLASSIFICATION OF THIS PAGE(When Data Entered)

Boundary conditions can be formulated in terms of one space variable, and this class of boundary value problems is solved through a numerical procedure. Included in the response is the influence of environmental dilation, which may be caused by a uniform temperature change and/or moisture adsorption. An example problem indicates the potential of rosette construction to drastically reduce stress concentration factors and illustrates significant errors resulting from improper modeling of the material structure.

UNCLASSIFIED

SECURITY CLASSIFICATION OF THIS PAGE(When Data Entered)

FOREWORD

This report was submitted by the Mechanics & Surface Interactions Branch, Nonmetallic Materials Division, Air Force Materials Laboratory, Air Force Wright Aeronautical Laboratories, Air Force Systems Command, Wright-Patterson Air Force Base, Ohio. The work was performed under Project 2279, Job Order 22790102. N. J. Pagano (AFML/MBM) was the laboratory project engineer.

This report covers work conducted in-house during the period of October 1975 to March 1976.

The author wishes to express his appreciation to Mr. L. E. Whitford and Sgt. J. Howett for the computer analysis and programming associated with this work.

ACCESSION for	
NTIS	White Section <input checked="" type="checkbox"/>
DDC	Buff Section <input type="checkbox"/>
UNANNOUNCED	<input type="checkbox"/>
JULIATION	
NOTES	
A	

D B C
RECEIVED
OCT 19 1976
REGULATORY
D

TABLE OF CONTENTS

SECTION		PAGE
I	INTRODUCTION	1
II	GEOMETRIC RELATIONS	2
III	STRESS ANALYSIS	6
IV	SOLUTION OF THE BOUNDARY VALUE PROBLEM	11
V	SAMPLE PROBLEM	13
VI	CONCLUSIONS	15
	APPENDIX	16
	REFERENCES	21

LIST OF ILLUSTRATIONS

FIGURE		PAGE
1	Geometric Configuration	22
2	Relation Between Adjacent Spirals	23
3	Differential Geometry	24
4	Initial and Final Sheet Configurations	25
5	Coordinate Systems	26
6	Hoop Stress Distribution	27
7	Axial Stress Distribution	28
8	Shear Stress Distribution	29
9	Radial Stress Distribution	30

SECTION I INTRODUCTION

One of the more popular approaches being employed in rocket nozzle structures is known as rosette construction. In this construction, layers of woven fabric composite materials are wrapped to follow spiral trajectories in the cross-section of an exit cone while the warp or fill direction generates a helix about the longitudinal axis of the structure. The purpose of rosette construction is to impart a high stiffness in the radial (thickness) direction as a means of improving load-carrying capacity as well as erosion resistance as compared to tangential wrapping of the layers.

The concept of rosette construction was initially devised for use in connection with ablative plastic liners, where structural performance was of minor interest. Consequently, no disciplined efforts were undertaken to relate the structural response to the established effective moduli of the basic sheet material. The concept is now being applied in the construction of rocket nozzle exit cones, where the structural response characteristics are critically important.

In this work, we shall develop the treatment defining the exact relations that exist among the various geometric parameters in a rosette cylinder. We shall also formulate the exact differential equations (in the sense of classical anisotropic elasticity theory) which define the mechanical response of such bodies under typical loading conditions imposed during an experimental characterization program. The governing equations will be solved numerically and examples presented which highlight the errors involved in the use of crude analytical techniques. It will be shown that, in general, 21 elastic coefficients are necessary to define the response of a rosette cylinder. Furthermore, the 21 coefficients are functions of position in the medium. While these elastic coefficients are not mutually independent since they are related to the stiffness matrix of the basic sheet material, they must all be included in the theory to define rigorous solutions of boundary value problems. Indeed,

even the proper interpretation of "simple" experiments, such as axial loading, torsion, and internal pressure depends upon such solutions. As such experiments are fundamental with respect to the structural design procedure, they define the scope of the present work. Included in the treatment will be the influence of uniform "expansional" strains [1] which allow us to consider the stress fields induced by uniform temperature changes, fabrication curing conditions, and absorption of swelling agents. We might also suggest that this work is basic to the problem of optimization of the material and geometric parameters in structural elements, such as rosette cylinders or conical shells.

SECTION II GEOMETRIC RELATIONS

The rosette pattern can be generated by starting with the basic sheet material in which the axes of elastic symmetry are denoted by x_i ($i = 1, 2, 3$) as shown in Figure 1(a). The sheet is then distorted to follow a certain cylindrical spiral trajectory, defined by C and C' , while the deformed axis x_1 assumes the helical path shown in Figure 1(b). The next sheet, initially oriented as in Figure 1(a), is then laid adjacent to the first and the process is continued until the entire area A between radii r_1 and r_0 is completely filled. As the specific equation of curve C is not known a priori, we must define the pertinent relations existing among the arc length, ply thickness, and inner and outer radii to establish this unique relation, consistent with the continuity requirement (complete filling of cross-sectional area A with no gaps). Finally, in order to develop the appropriate constitutive relations, the path of the original x_1 axis within the rosette cylinder must be defined.

We begin by treating the trajectory of curve C . Consider two arbitrary spirals C and C' which intersect a circle of radius r at points A and D as shown in Figure 2. For conceptual purposes, we may let the two spirals represent the edges of a single layer of the basic sheet material, which we assume is completely flexible. Thus, the perpendicular distance between

the two spirals, t , must be a constant. Let the local angles between the tangents to the spirals at A and B and the intersecting circles centered at O be denoted by α and α' , respectively. We shall henceforth refer to α as the arc angle. Our convention is that the angle α is measured in the clockwise direction from the local positive θ direction to the spiral tangent. By applying the law of sines to the triangle OAB, we get

$$r \sin \alpha = r' \sin \alpha' \quad (1)$$

Since there is not a unique trajectory of curve C satisfying the continuity requirement, we select the class of curves commonly employed in rosette construction, namely, the one in which all curves intersect a circle of given radius at the same arc angle. Therefore, at radial distance r' , the arc angle on C is equal to α' . Hence, the parametric form of the equation¹ of curve C is given by (1), or

$$r \sin \alpha = r_o \sin \alpha_o = \text{const.} \quad (2)$$

where α_o represents the arc angle corresponding to the point (r_o, θ_o) in polar coordinates.

To continue our study of the spiral configuration, we consider the differential geometric relation (see Figure 3)

$$dr = -r \tan \alpha d\theta \quad (3)$$

Eliminating the dependence on r in favor of α through (2) and (3), and integrating yields

$$\theta - \theta_o = \alpha_o + \cot \alpha_o - \alpha - \cot \alpha \quad (4)$$

And finally, using (2) again, we can express the equation of C in terms of polar coordinates as

$$\theta - \theta_o = \alpha_o + \cot \alpha_o - \sin^{-1} \left(\frac{r_o \sin \alpha_o}{r} \right) \mp \frac{(r^2 - r_o^2 \sin^2 \alpha_o)^{1/2}}{r_o \sin \alpha_o} \quad (5)$$

¹ This equation, as well as several others presented in this section have been derived by Mamrol [2] using a different approach.

where the ambiguous sign is negative if $0 < \alpha_0 < \pi/2$ and positive if $\pi/2 < \alpha_0 < \pi$.

In order to fabricate the rosette, we need to compute the arc length of the spiral. From Figure 3, we observe that infinitesimal arc length ds is given by

$$ds = \frac{-dr}{\sin \alpha} \quad (6)$$

Substituting for dr from (2) into (6) and integrating, we get

$$s = \frac{r_0}{2 \sin \alpha_0} \left(1 - \frac{\sin^2 \alpha_0}{\sin^2 \alpha} \right) \quad (7)$$

or

$$s = \frac{r_0}{2 \sin \alpha_0} \left(1 - \frac{r^2}{r_0^2} \right) \quad (8)$$

both of which represent the arc length from (r_0, θ_0) to an arbitrary point (r, θ) .

In order to define the relation between two arbitrary spirals, we again return to Figure 2, noting that

$$t \sin \alpha' = r \sin (\alpha - \alpha') \quad (9)$$

by use of the law of sines. Solving (9) for α' gives

$$\cot \alpha' = \cot \alpha + \frac{t}{r \sin \alpha} \quad (10)$$

By applying (4) to points D and B and taking the difference, we find that

$$\Psi = \alpha' + \cot \alpha' - \alpha - \cot \alpha \quad (11)$$

Thus the central angle Φ subtended by arc AD is given by

$$\Phi = \frac{t}{r \sin \alpha} = \frac{t}{r_0 \sin \alpha_0} \quad (12)$$

where the last step follows from (2). Noting that $r_o \sin \alpha_o$ is a constant, we see that the central angle subtended by the radii through two points which lie on two given spirals, the points being at the same radial distance from O, is constant. Therefore, given the trajectory of one spiral within the rosette pattern, any other spiral is generated by a rigid body rotation about the longitudinal axis through point O. The magnitude of the angle of rotation is given by (12), where t is the perpendicular distance separating the spirals. Hence, the number of layers N within the cylinder is

$$N = \frac{2\pi r_o \sin \alpha_o}{t_1} \quad (13)$$

where t_1 is the thickness of a single layer. Satisfaction of Eqs. (13) and (4) or (5) implies satisfaction of the continuity requirement. Finally, given the equation of one spiral, i.e., (4), the equation of any arbitrary spiral can be expressed as

$$\theta - \theta_o - \Phi = \alpha_o + \cot \alpha_o - \alpha - \cot \alpha \quad (14)$$

where Φ depends on dimension t through Eq. (12).

In order to relate the helical angle ω to the respective angle in the basic sheet, Φ , we refer to Figure 4, where the basic sheet is illustrated in 4(a) and the top view of the sheet in the rosette cylinder is shown in 4(b). First, we observe the relation

$$z = \xi \cot \phi \quad (15)$$

where ξ can be evaluated from (8). Thus, we get

$$z = \frac{(r_o^2 - r^2) \cot \phi}{2r_o \sin \alpha_o} \quad (16)$$

Now, helical angle ω is defined by

$$\cos \omega = \frac{dz}{dR} \quad (17)$$

where dR is the infinitesimal arc length along the deformed line QP in the rosette cylinder, so that

$$dR^2 = dz^2 + dr^2 + r^2 d\theta^2 \quad (18)$$

Taking differentials of (4) and (16), using (2), and substituting the results into (18) gives

$$dR = \frac{-r dr}{r_o \sin \alpha_o \sin \phi} \quad (19)$$

Use of (17) and (19), in conjunction with the evaluation of dz from (16) yields

$$\cos \omega = \cos \phi \quad (20)$$

Hence, in the transformation of the basic sheet into the rosette pattern, angles with respect to the longitudinal direction are preserved. This implies that the angle between line segments in the basic sheet intersecting at an arbitrary point F is carried into the identical angle between the corresponding tangents at F' through the present transformation, where F' is the transformed position of F .

SECTION III STRESS ANALYSIS

In this section, we shall study the elastic response of a rosette cylinder under the application of an axisymmetric loading system, such as that usually imposed in experimental characterization, in addition to uniform expansional strains [1]. The latter permit the treatment of thermal stresses induced by uniform temperature changes, curing stresses [3,4], and swelling stresses caused by absorption of fluid. We assume that the stress field is independent of the axial coordinate z . Thus, the localized disturbances near the ends of the specimen under imposed displacement boundary conditions are excluded in the present work. As mentioned earlier, the rosette cylinder is constructed of numerous layers of a composite material. In what follows, each layer is treated as a homogeneous, anisotropic material characterized by its effective moduli [5]. Thus the mechanical properties which govern the response are

the effective stiffness coefficients and expansional strains of the basic sheet material. In practical applications, the basic sheet material is orthotropic (9 elastic moduli and 3 expansional strains), so we shall consider this material class in the present work, although treatment of materials possessing arbitrary anisotropy can be incorporated without difficulty.

It is important to recall that the rosette structure involves a system of layers, the trajectories of which are mutually related via rigid body rotations. Furthermore, the helical angles defined by the various spiral layers are all identical. These facts imply that the material structure is axisymmetric, i.e., while the moduli are functions of radial position, they are independent of θ . As the loading is also axisymmetric, the most convenient coordinate system to employ in connection with the stress analysis is that of cylindrical coordinates r, θ, z , rather than coordinates defined by the spiral trajectories.

The stress components in the present class of boundary value problems are functions of radial position only. It follows that the strain distribution will only be a function of r . By use of the strain-displacement relations of linear elasticity, i.e.,

$$\begin{aligned} \epsilon_r &= u, r, \quad \epsilon_\theta = \frac{1}{r} (u + v, \theta), \quad \epsilon_z = w, z \\ \gamma_{r\theta} &= v, r + \frac{1}{r} (u, \theta - v), \quad \gamma_{rz} = u, z + w, r, \quad \gamma_{z\theta} = v, z + \frac{1}{r} w, \theta \end{aligned} \quad (21)$$

where u, v , and w represent the r, θ , and z components of displacement, respectively, and commas denote differentiation, it can be shown that the general form of the displacement field² is given by

$$\begin{aligned} u &= U(r) \\ v &= Arz + V(r) \\ w &= ez + W(r) \end{aligned} \quad (22)$$

²We assume that the displacement field is continuous, i.e., there are no slits in the cylinder.

where e and A are constants. By substituting (22) into (21), the strain field can be expressed as

$$e_r = U, r, \quad e_\theta = U/r, \quad e_z = e \quad (23)$$

$$\gamma_{r\theta} = V, r - V/r, \quad \gamma_{rz} = W, r, \quad \gamma_{z\theta} = Ar$$

The stress equations of equilibrium for axisymmetric problems take the form

$$\begin{aligned} \sigma_{r,r} + \frac{1}{r}(\sigma_r - \sigma_\theta) &= 0 \\ r_{rz,r} + \frac{1}{r} r_{rz} &= 0 \\ r_{r\theta,\theta} + \frac{2}{r} r_{r\theta} &= 0 \end{aligned} \quad (24)$$

Rewriting the first of (24) and integrating the last two directly yields

$$\begin{aligned} (r\sigma_r), r &= \sigma_\theta \\ r r_{rz} &= \text{const.} \quad \equiv B \\ r^2 r_{r\theta} &= \text{const.} \quad \equiv D \end{aligned} \quad (25)$$

The governing field equations are thus defined by (23), (24), and the constitutive equations, i.e.,

$$\sigma_{ij} = C_{ijkl}(e_{kl} - e_{kl}) \quad (26)$$

where e_{kl} are the components of the mathematical strain tensor, in contrast to those of (23) in which the shear strain components are engineering strains, and e_{kl} are the components of the mathematical expansional strain tensor.

In order to develop the proper form of the rosette stiffness coefficients, we refer to the orthogonal coordinate systems shown in Figure 5. Coordinates $x_i (i=1, 2, 3)$ are oriented along the axes of elastic symmetry of the basic sheet

material, \bar{x}_i are tangent and normal to an arbitrary spiral path, and x_i' are the cylindrical coordinate axes θ, r, z , where each coordinate system is right-handed. Letting x_i and y_i represent two arbitrary orthogonal coordinate systems and C_{ijkl} and B_{ijkl} the respective stiffness coefficients in the two systems, the transformation equations are given by

$$B_{ijkl} = a_{pi} a_{qj} a_{rk} a_{sl} C_{pqrs} \quad (27)$$

where a_{ij} is the cosine of the angle between x_i and y_j . The stiffness coefficients in the x_i' system, C_{ijkl}' , may thus be computed by applying (27) for the transformation from x_i to \bar{x}_i , followed by that from \bar{x}_i to x_i' . The results of these transformations are given in the appendix. It will suffice at this point to state that, in general, all elements of C_{ijkl}' are non-zero, but they may all be computed in terms of the (nine) stiffness coefficients of the basic sheet material, C_{ijkl} . Finally, to save writing, we shall subsequently employ the standard contracted notation [6] to represent the stiffness coefficients in terms of double indices, e.g., C_{ij} . Thus, the 9 independent components C_{ij} transform into 13 non-zero components \bar{C}_{ij} , which in turn are carried into 21 components C_{ij}' . The constitutive relations now assume the form

$$\begin{pmatrix} \sigma_\theta \\ \sigma_r \\ \sigma_z \\ r_{rz} \\ r_{z\theta} \\ r_{r\theta} \end{pmatrix} = \begin{pmatrix} C_{11}' & C_{12}' & C_{13}' & C_{14}' & C_{15}' & C_{16}' \\ & C_{22}' & C_{23}' & C_{24}' & C_{25}' & C_{26}' \\ & & C_{33}' & C_{34}' & C_{35}' & C_{36}' \\ \text{SYMM.} & & & C_{44}' & C_{45}' & C_{46}' \\ & & & & C_{55}' & C_{56}' \\ & & & & & C_{66}' \end{pmatrix} \begin{pmatrix} U/r - e_\theta \\ U_{,r} - e_r \\ e - e_z \\ W_{,r} - e_{rz} \\ Ar - e_{z\theta} \\ V_{,r} - V/r - e_{r\theta} \end{pmatrix} \quad (28)$$

where

$$C'_{ij} = C'_{ij}(r) \quad (29)$$

The expansional strain components, denoted by the symbol e , are also functions of r (except for e_z , which is a constant) and are related to the sheet expansional strains e_i ($i=1,2,3$) through the standard transformation of (engineering) strain equations (see appendix). For the case of thermal expansion, the latter strains are given by

$$e_i = \alpha_i T \quad (30)$$

where α_i are the coefficients of linear thermal expansion and T is the difference between ambient temperature and that in the stress-free state. For fluid absorption, e_i are defined by

$$e_i = \beta_i m \quad (31)$$

where β_i are the free swelling strain components per unit volume of fluid in the medium, while m is the total volume of fluid absorbed.

Upon evaluating the stiffness coefficients C'_{ij} and substituting (28) into (25), we obtain 3 ordinary differential equations in terms of dependent variables U, V , and W . Introducing the expression

$$\beta = \frac{r_o \sin \alpha_o}{r} \quad (32)$$

these governing field equations become

$$\begin{aligned} G_3 r U_{,rr} + G_2 U_{,r} + G_1 U/r + G_7 r V_{,rr} + G_6 (V_{,r} - V/r) + G_5 r W_{,rr} \\ + G_4 W_{,r} = G_8 + G_o e + G_9 Ar \end{aligned} \quad (33)$$

$$C'_{24} U_{,r} + C'_{14} U/r + C'_{46} (V_{,r} - V/r) + C'_{44} W_{,r} = H_1 + B/r + \bar{C}_{35} \beta e + (\bar{C}_{55} - \bar{C}_{44}) A \beta r (1 - \beta^2)^{1/2}$$

$$C'_{26} U_{,r} + C'_{16} U/r + C'_{66} (V_{,r} - V/r) + C'_{46} W_{,r} = (G_8 + G_o e) \beta (1 - \beta^2)^{1/2} - C'_{56} Ar + D/r^2$$

in the region $r_1 \leq r \leq r_o$. The various coefficients in (33) are, in general, functions of r and are given in the appendix.

The boundary conditions required to complete the definition of the present boundary value problem are given by

$$\begin{aligned}\sigma_r(r_o) &= \sigma_o & V(a) &= V_o \\ \sigma_r(r_1) &= \sigma_1 & W(b) &= W_o\end{aligned}\tag{34}$$

where σ_o , σ_1 , V_o , and W_o are prescribed constants, and a and b are arbitrary values of r within the medium. The constants V_o and W_o are simply required to define the rigid body displacement components. Finally, the constants e , A , B , and D must be prescribed. Note that B and D completely define shear stresses r_{rz} and $r_{r\theta}$ according to (25) and that the latter normally vanish under typical experimental loading conditions.

The remaining quantities of interest are the axial force P_o and torque T_o , which can be expressed as

$$\begin{aligned}P_o &= 2\pi \int_{r_1}^{r_o} \sigma_z r dr \\ T_o &= 2\pi \int_{r_1}^{r_o} r_{z\theta} r^2 dr\end{aligned}\tag{35}$$

The method of solution adopted here requires the prescription of e and A , rather than applied loads P_o and T_o . However, solutions for specified values of P_o and T_o can be developed through a simple influence function approach.

SECTION IV SOLUTION OF THE BOUNDARY VALUE PROBLEM

The complexity of the coefficients involved in field equations (33), in particular, the appearance of the irrational functions, precludes efficient application of the standard series methods of solution for ordinary differential

equations. Consequently, we have adopted the finite-difference approach, incorporating the use of higher order difference representations. Forward differences have been utilized throughout the solution with a maximum of 4 nodal point functions being employed in the difference approximation. Since the first of (33) involves second derivatives of the displacement functions and we wish to satisfy the field equations at all points in the region, including the boundaries, we have expanded the region by adding two nodal points outside the right hand boundary $r = r_0$.

Consider the series of equi-spaced nodal points $x = 0, h, 2h, 3h$, or $x_i = ih$ ($i=0, 1, 2, 3$) where $x_0 = r_0$ and d is a constant. Letting y represent an arbitrary function of x (or r) and letting $y_i = y(x_i)$, we approximate the first and second derivatives of y , in the event that all 4 nodal points lie in the (expanded) region, by

$$\begin{aligned} hy'_0 &\cong -\frac{11}{6} y_0 + 3y_1 - \frac{3}{2} y_2 + \frac{1}{3} y_3, \\ h^2 y''_0 &\cong 2y_0 - 5y_1 + 4y_2 - y_3, \end{aligned} \quad \begin{aligned} r &\leq r_0 - h \end{aligned} \quad (36)$$

where primes denote derivatives. Equations (36) are easily derived by expanding y_1, y_2, y_3 in Taylor series about y_0 , truncating each series after the cubic term in h , and then solving for y'_0 and y''_0 . At $r = r_0$, three point difference approximations are employed

$$\begin{aligned} h y'_0 &\cong -\frac{3}{2} y_0 + 2y_1 - \frac{1}{2} y_2, \\ h^2 y''_0 &\cong y_0 - 2y_1 + y_2, \end{aligned} \quad \begin{aligned} r &= r_0 \end{aligned} \quad (37)$$

and finally, at $r = r_0 + h$, we put

$$h y'_0 \cong y_1 - y_0, \quad r = r_0 + h \quad (38)$$

Thus, letting N represent the total number of nodal points employed to subdivide the expanded region, we write the finite-difference approximation of the first of (33) at $N-2$ nodal points and that of the second and third of (33) at $N-1$ points. Applying the finite-difference representations of the traction boundary conditions in (34) after substituting the expression for σ_r given by (28) and the two conditions for V and W from (34), we arrive at $3N$ equations to be solved for the $3N$ unknowns, i.e., U, V , and W at the N nodal points. Utilizing a computer routine for sparsely populated matrices, the solution of a given problem is executed in a matter of seconds on a CDC6600.

Upon solving for the nodal displacement functions, the stress and strain fields are defined through the use of eqs. (28) and (23), respectively, where derivatives are evaluated via the appropriate relation among (36)-(38). Since the solution technique is an approximate one, the degree of approximation may be assessed by writing a system of "check" equations, consisting of (25), the compatibility relation,

$$e_r = e_\theta + r e_{\theta, r} \quad (39)$$

and the identity

$$\int_{r_1}^{r_0} \sigma_\theta dr = r_0 \sigma_\theta - r_1 \sigma_\theta \quad (40)$$

which represents the integral of the first of (25).

SECTION V SAMPLE PROBLEM

In this section we shall consider the stress field within a rosette cylinder in which the basic sheet material is a high modulus unidirectional graphite/epoxy composite. Letting x_1 represent the direction parallel to the fibers, we assume the following basic sheet moduli (psi),

$$\begin{aligned} C_{11} &= 20.2 \times 10^6, & C_{12} &= C_{13} = 4.72 \times 10^5 \\ C_{23} &= 3.84 \times 10^5, & C_{22} &= C_{33} = 1.50 \times 10^6 \end{aligned} \quad (41)$$

$$C_{44} = 5.60 \times 10^5, \quad C_{55} = C_{66} = 7.0 \times 10^5 \quad (41 \text{ cont.})$$

The cylinder is under an internal pressure $\sigma_1 = -1000$ psi, while $\sigma_o = B = D = 0$, i.e., the outer surface is traction-free and the shear traction on the inner surface vanishes. We also let $e = A = 0$, which imply that axial force P_o and torque T_o , in general, are different from zero. The inner and outer radii are 3" and 4", respectively, and the expansional strains e_i are assumed to vanish.

Three specific material configurations will be treated. In the first (rosette), we put $\alpha_o = \pi/12$ and $\phi = \pi/3$. Two other configurations which may be employed to crudely approximate the rosette structure have also been considered. These are represented by the parameters $\alpha_o = 0$, $\phi = \pi/3$ (helical-wound cylinder) and $\alpha_o = 0$, $\phi = \pi/2$ (hoop-wound cylinder). In the latter two configurations, exact solutions for the present class of boundary value problems are available (see [7]). Such solutions were also treated by use of the present approach to serve in checking the computer code. In the results presented here, 403 node points were utilized in each solution, which is sufficient to achieve a precision of approximately 4 significant figures for the computed stress components.

Distributions of the four non-vanishing stress components, σ_θ , σ_z , $r_{z\theta}$, and σ_r , throughout the domain are given in Figures 6-9 for the foregoing 3 configurations. Clearly, the helical-wound and hoop-wound cylinder models represent very poor approximations to the actual response, although smaller errors than those indicated here may be expected in systems of less extreme anisotropy than the present case. From these curves, we also observe that the rosette structure effects a considerable smoothing of the stress field, at least under the conditions treated here, i.e., stress concentrations in σ_θ , σ_z , and $r_{z\theta}$ are close to unity. While the cylindrical (r, θ, z) components of the stress tensor are not particularly informative with regard to failure prediction in orthotropic bodies, the stress components in the elastic symmetry coordinates x_i (see Figure 5) can be easily determined through the

standard stress transformation equations. Consequently, coupled with an appropriate failure criterion for the basic sheet material, the present solution provides a means of optimizing the material and geometric parameters in rosette cylindrical bodies under axisymmetric loading.

SECTION VI CONCLUSIONS

We have derived the pertinent relations which describe the geometry of the spiral paths traversed by the layers within a rosette cylindrical body. It has been demonstrated that prescription of inner and outer radii, r_i and r_o , respectively, arc angle α at one point, and layer thickness t_l completely defines the appropriate geometric pattern. The spiral trajectories of the various layer interfaces are interrelated through simple rigid body rotations, while helical angle ϕ is constant. These facts imply axisymmetry of the distribution of heterogeneous effective stiffness coefficients C'_{ij} .

Taking advantage of the axisymmetric material structure, we have formulated the governing equations of elasticity for the rosette cylinder under boundary conditions and expansional strains which are independent of θ . Although the stiffness coefficient matrix C'_{ij} is fully populated (21 constants) in general, these coefficients only depend upon the (orthotropic) moduli of the basic sheet material and the angles α and ϕ . The finite-difference method has led to the development of an efficient computer program for the general solution of the axisymmetric class of boundary value problems. An example solution has demonstrated the tremendous smoothing influence of the rosette construction on the elastic stress field, which will be an important feature of this concept in structural applications.

APPENDIX

The \bar{x}_i components of the stiffness matrix (see Figure 5) are defined by substituting

$$a_{11} = a_{23} = \sin \phi = N, \quad a_{13} = -a_{21} = \cos \phi = M, \quad a_{32} = -1 \quad (A-1)$$

$$a_{12} = a_{22} = a_{31} = a_{33} = 0$$

into (27). Upon switching to standard contracted notation, we get

$$\begin{aligned} \bar{C}_{11} &= C_{11}N^4 + C_{22}M^4 + 2(C_{12} + 2C_{66})M^2N^2 \\ \bar{C}_{12} &= C_{13}N^2 + C_{23}M^2 \\ \bar{C}_{13} &= (C_{11} + C_{22} - 4C_{66})M^2N^2 + C_{12}(M^4 + N^4) \\ \bar{C}_{15} &= [C_{11}N^2 - C_{22}M^2 + (C_{12} + 2C_{66})(M^2 - N^2)] MN \\ \bar{C}_{22} &= C_{33} \\ \bar{C}_{23} &= C_{13}M^2 + C_{23}N^2 \\ \bar{C}_{25} &= (C_{13} - C_{23})MN \\ \bar{C}_{33} &= C_{11}M^4 + C_{22}N^4 + 2(C_{12} + 2C_{66})M^2N^2 \\ \bar{C}_{35} &= [C_{11}M^2 - C_{22}N^2 + (C_{12} + 2C_{66})(N^2 - M^2)] MN \\ \bar{C}_{44} &= C_{55}M^2 + C_{44}N^2 \\ \bar{C}_{46} &= (C_{55} - C_{44})MN \end{aligned} \quad (A-2)$$

$$\bar{C}_{55} = (C_{11} + C_{22})M^2N^2 - 2C_{12}M^2N^2 + C_{66}(M^2 - N^2)^2 \quad (\text{A-2 cont.})$$

$$\bar{C}_{66} = C_{55}N^2 + C_{44}M^2$$

$$\bar{C}_{i4} = \bar{C}_{i6} = 0 \quad (i = 1, 2, 3, 5)$$

Similarly, the transformation from \bar{x}_i to x'_i , upon substituting

$$\begin{aligned} a_{11} = a_{22} = \cos \alpha &\equiv (1-\beta^2)^{1/2}, \quad a_{21} = -a_{12} = \sin \alpha \equiv \beta, \quad a_{33} = 1 \\ a_{13} = a_{23} = a_{31} = a_{32} &= 0 \end{aligned} \quad (\text{A-3})$$

into (27) yields

$$\begin{aligned} C'_{11} &= \bar{C}_{11}(1-\beta^2)^2 + \bar{C}_{22}\beta^4 + 2(\bar{C}_{12} + 2\bar{C}_{66})\beta^2(1-\beta^2) \\ C'_{12} &= (\bar{C}_{11} + \bar{C}_{22} - 4\bar{C}_{66})\beta^2(1-\beta^2) + \bar{C}_{12}(2\beta^4 - 2\beta^2 + 1) \\ C'_{13} &= \bar{C}_{13}(1-\beta^2) + \bar{C}_{23}\beta^2 \\ C'_{14} &= [(2\bar{C}_{46} - \bar{C}_{15})(1-\beta^2) - \bar{C}_{25}\beta^2] \beta \\ C'_{15} &= [\bar{C}_{15}(1-\beta^2) + (\bar{C}_{25} + 2\bar{C}_{46})\beta^2] (1-\beta^2)^{1/2} \\ C'_{16} &= [\bar{C}_{11}(\beta^2 - 1) + \bar{C}_{22}\beta^2 + (\bar{C}_{12} + 2\bar{C}_{66})(1-2\beta^2)] \beta(1-\beta^2)^{1/2} \\ C'_{22} &= \bar{C}_{11}\beta^4 + \bar{C}_{22}(1-\beta^2)^2 + 2(\bar{C}_{12} + 2\bar{C}_{66})\beta^2(1-\beta^2) \\ C'_{23} &= \bar{C}_{13}\beta^2 + \bar{C}_{23}(1-\beta^2) \\ C'_{24} &= [-\bar{C}_{15}\beta^2 + (\bar{C}_{25} + 2\bar{C}_{46})(\beta^2 - 1)] \beta \\ C'_{25} &= [(\bar{C}_{15} - 2\bar{C}_{46})\beta^2 + \bar{C}_{25}(1-\beta^2)] (1-\beta^2)^{1/2} \end{aligned} \quad (\text{A-4})$$

$$C'_{26} = [-\bar{C}_{11}\beta^2 + \bar{C}_{22}(1-\beta^2) + (\bar{C}_{12} + 2\bar{C}_{66})(2\beta^2 - 1)] \beta(1-\beta^2)^{1/2}$$

$$C'_{33} = \bar{C}_{33}$$

$$C'_{34} = -\bar{C}_{35}\beta$$

$$C'_{35} = \bar{C}_{35}(1-\beta^2)^{1/2}$$

$$C'_{36} = (\bar{C}_{23} - \bar{C}_{13})\beta(1-\beta^2)^{1/2}$$

$$C'_{44} = \bar{C}_{44}(1-\beta^2) + \bar{C}_{55}\beta^2$$

(A-4 cont.)

$$C'_{45} = (\bar{C}_{44} - \bar{C}_{55})\beta(1-\beta^2)^{1/2}$$

$$C'_{46} = [(\bar{C}_{15} - \bar{C}_{25})\beta^2 + \bar{C}_{46}(1-2\beta^2)] (1-\beta^2)^{1/2}$$

$$C'_{55} = \bar{C}_{44}\beta^2 + \bar{C}_{55}(1-\beta^2)$$

$$C'_{56} = [(\bar{C}_{25} - \bar{C}_{15})(1-\beta^2) + \bar{C}_{46}(1-2\beta^2)] \beta$$

$$C'_{66} = (\bar{C}_{11} + \bar{C}_{22} - 2\bar{C}_{12})\beta^2(1-\beta^2) + \bar{C}_{66}(1-2\beta^2)^2$$

where we have assumed that $\alpha \leq \pi/2$. Note that \bar{C}_{ij} in the above expressions are all constants.

Substituting (A-1) and (A-3) into the standard strain transformation equations leads to

$$\begin{aligned} e_{\theta} &= (e_3 - e_1 N^2 - e_2 M^2)\beta^2 + e_1 N^2 + e_2 M^2 \\ e_r &= (e_1 N^2 + e_2 M^2 - e_3)\beta^2 + e_3 \\ e_z &= e_1 M^2 + e_2 N^2 \end{aligned} \quad (A-5)$$

$$e_{rz} = 2(e_2 - e_1)MN\beta$$

$$e_{z\theta} = 2(e_1 - e_2)MN(1-\beta^2)^{1/2} \quad (A-5 \text{ cont.})$$

$$e_{r\theta} = 2(e_3 - e_1 N^2 - e_2 M^2)\beta(1-\beta^2)^{1/2}$$

where we recall that e_{θ} --- are the engineering expansional strain components.

Finally, the remaining functions appearing in field equations (33) are given by

$$G_0 = \bar{C}_{13} - \bar{C}_{23}$$

$$G_1 = 3F_1\beta^4 - 2F_2\beta^2 - \bar{C}_{11}$$

$$G_2 = \bar{C}_{22} - \bar{C}_{11} - G_1$$

$$G_3 = F_1\beta^4 - 2F_2\beta^2 + \bar{C}_{22} \quad (A-6)$$

$$G_4 = (F_3\beta^2 + \bar{C}_{15} - 2\bar{C}_{46})\beta$$

$$G_5 = -(F_3\beta^2 + \bar{C}_{25} + 2\bar{C}_{46})\beta$$

$$G_6 = [-3F_1\beta^4 + (F_1 + 3F_2)\beta^2 + \bar{C}_{11} - \bar{C}_{22}]\beta(1-\beta^2)^{-1/2}$$

$$G_7 = (-F_1\beta^2 + F_2)\beta(1-\beta^2)^{1/2}$$

$$G_8 = (\bar{C}_{12} - \bar{C}_{11})(e_1 N^2 + e_2 M^2) + (\bar{C}_{22} - \bar{C}_{12})e_3 + (\bar{C}_{23} - \bar{C}_{13})(e_1 M^2 + e_2 N^2)$$

$$+ 2(\bar{C}_{25} - \bar{C}_{15})(e_1 - e_2)MN$$

$$G_9 = (-2F_3\beta^2 + \bar{C}_{15} - 2\bar{C}_{25})(1-\beta^2)^{-1/2}$$

(A-6 cont.)

$$H_1 = -[\bar{C}_{15}(e_1 N^2 + e_2 M^2) + \bar{C}_{25}e_3 + \bar{C}_{35}(e_1 M^2 + e_2 N^2) + 2\bar{C}_{55}(e_1 - e_2)MN]\beta$$

where

$$F_1 = \bar{C}_{11} + \bar{C}_{22} - 2\bar{C}_{12} - 4\bar{C}_{66}$$

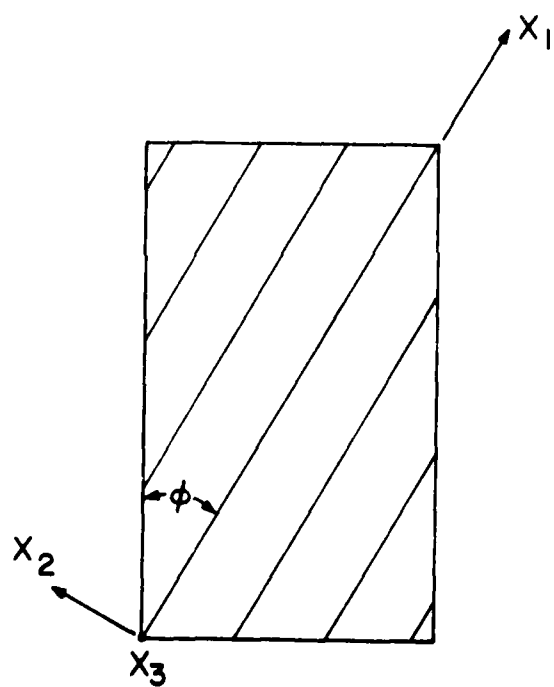
$$F_2 = \bar{C}_{22} - \bar{C}_{12} - 2\bar{C}_{66} \quad (A-7)$$

$$F_3 = \bar{C}_{15} - \bar{C}_{25} - 2\bar{C}_{46}$$

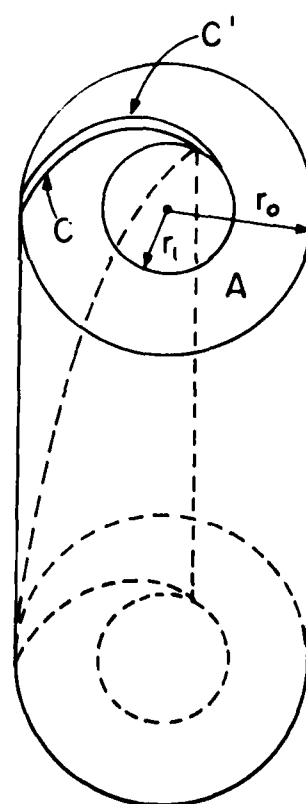
This completes the definition of all functions appearing in the governing field equations (33).

REFERENCES

1. J.C. Halpin and N.J. Pagano, "Consequences of Environmentally Induced Dilatation in Solids," Recent Advances in Engineering Science (A.C. Eringen, ed.), Gordon and Breach, New York, 1970, pp. 33-46.
2. F.E. Mamrol, Geometric Design Data-Rosette Lay-up, Rpt. 64SD262, Aug. 1964, General Electric, King of Prussia, PA.
3. H.T. Hahn and N.J. Pagano, "Curing Stresses in Composite Laminates," Journal of Composite Materials, Vol. 9, Jan. 1975, pp. 91-106.
4. N.J. Pagano, H.T. Hahn and R. Kuhbänder, "Experimental Determination of Composite Curing Stresses," ASTM Fourth Conference on Composite Materials: Testing and Design, May 1976, Valley Forge, PA.
5. Z. Hashin, "Theory of Mechanical Behavior of Heterogeneous Media," Applied Mechanics Reviews, Vol. 17, Jan. 1964, pp. 1-9.
6. R.F.S. Hearmon, Applied Anisotropic Elasticity, Oxford, London, and New York, 1961.
7. N.J. Pagano and J.M. Whitney, "Geometric Design of Composite Cylindrical Characterization Specimens," Journal of Composite Materials, Vol. 4, July 1970, pp. 360-378.



(a)



(b)

Figure 1. Geometric Configuration

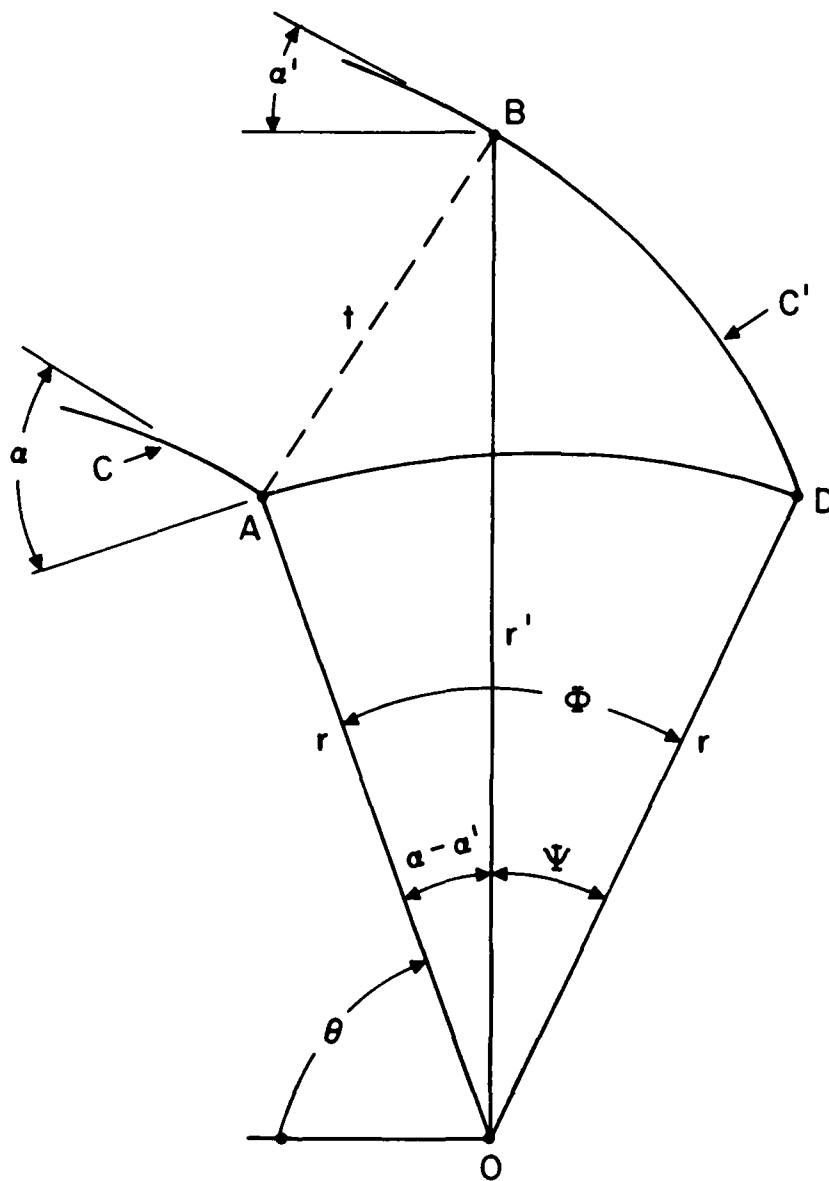


Figure 2. Relation Between Adjacent Spirals

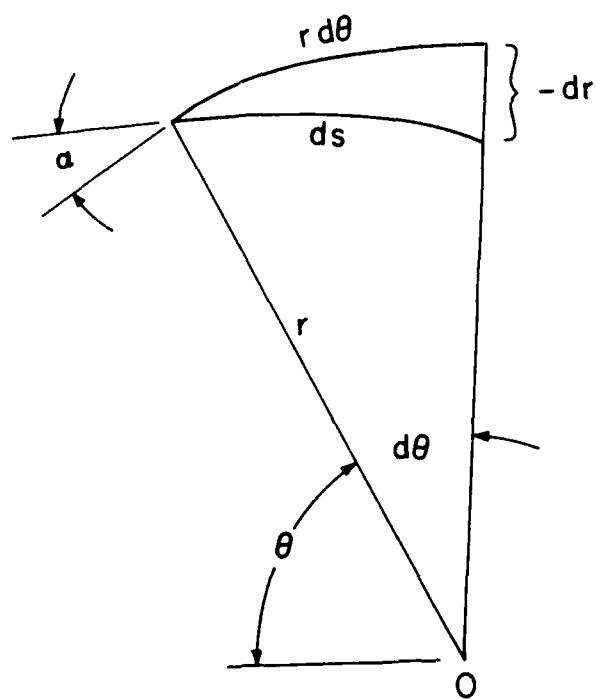
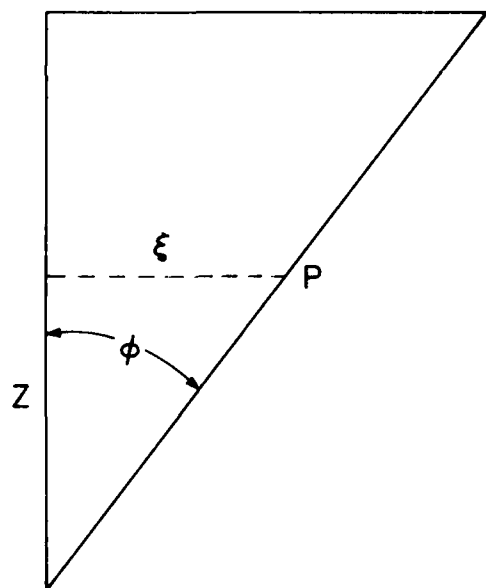
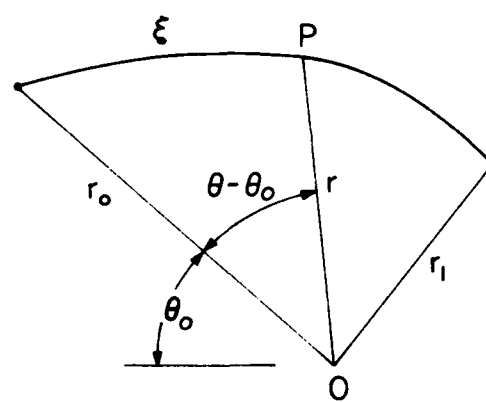


Figure 3. Differential Geometry

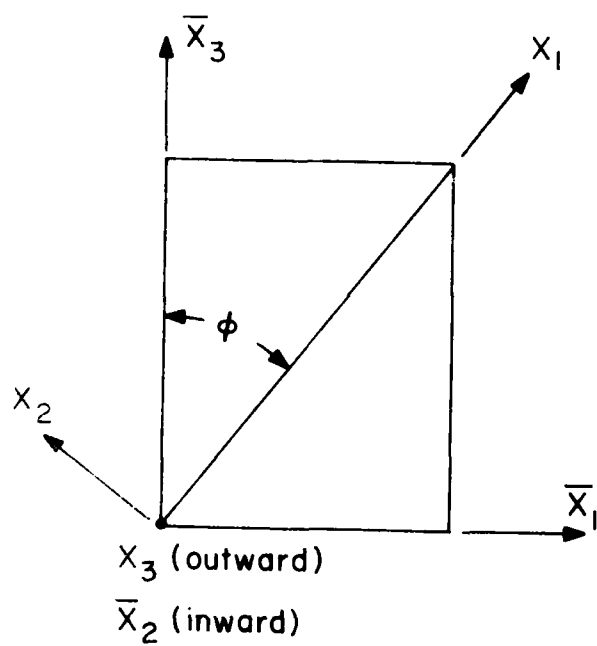


(a)

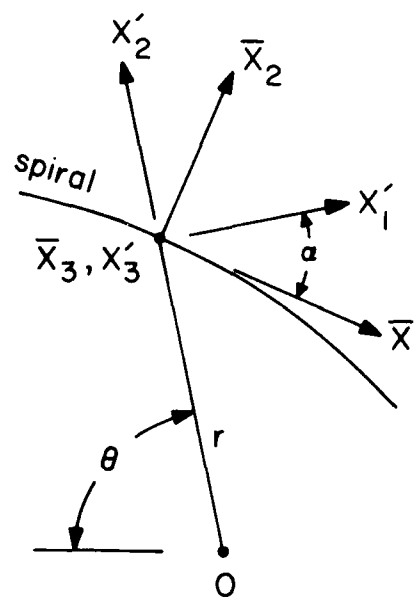


(b)

Figure 4. Initial and Final Sheet Configurations



(a)



(b)

Figure 5. Coordinate Systems

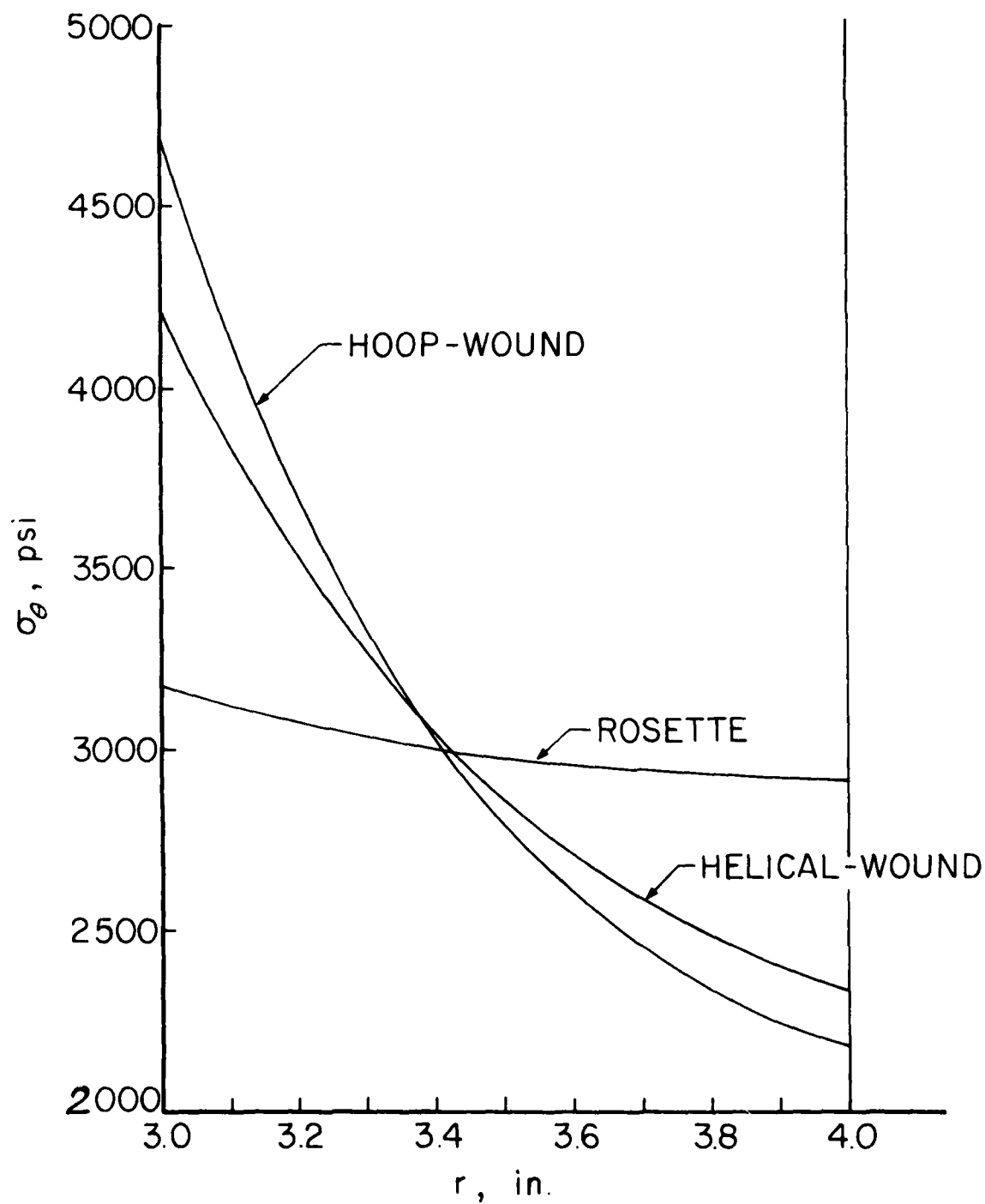


Figure 6. Hoop Stress Distribution

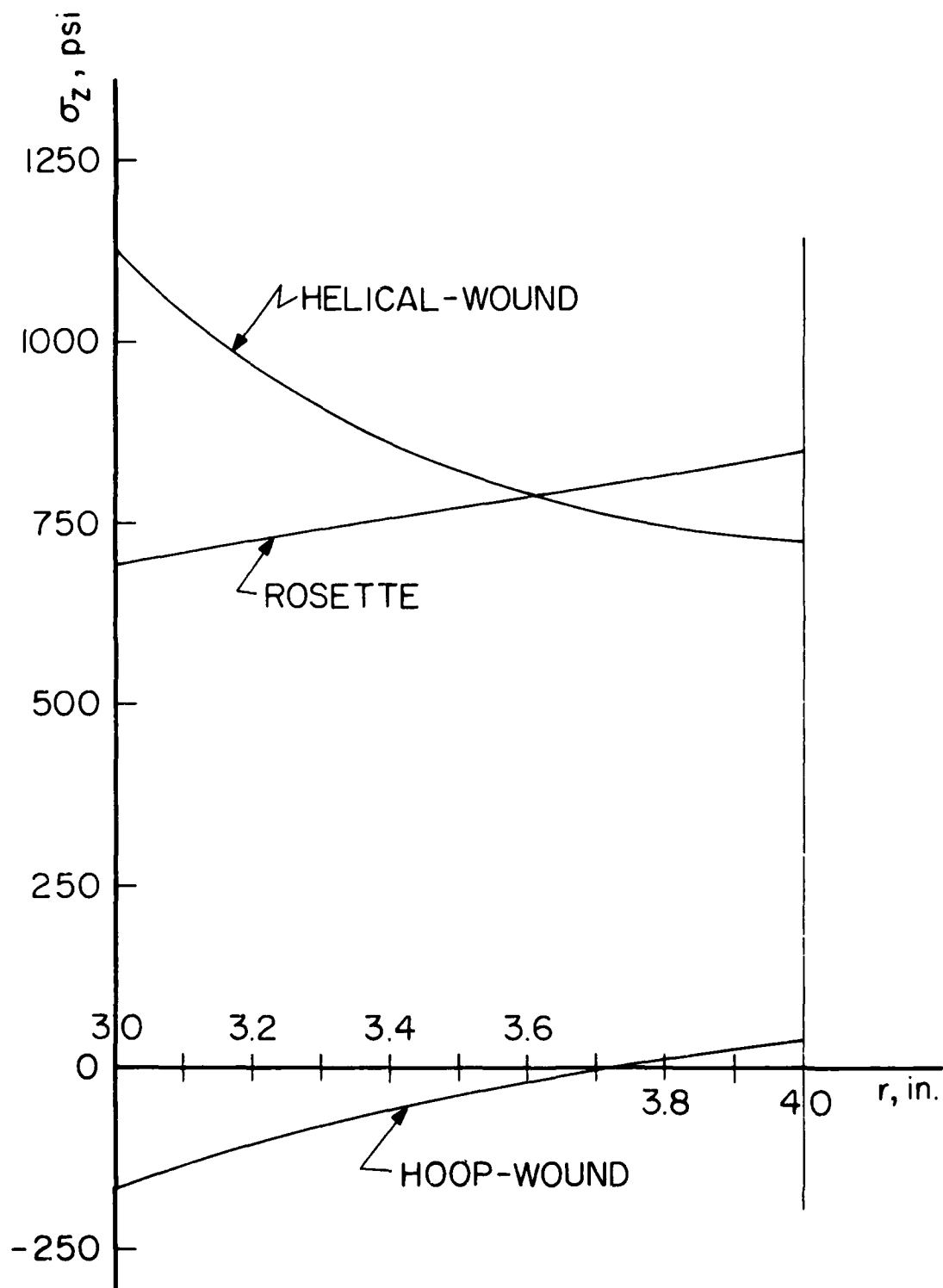


Figure 7. Axial Stress Distribution

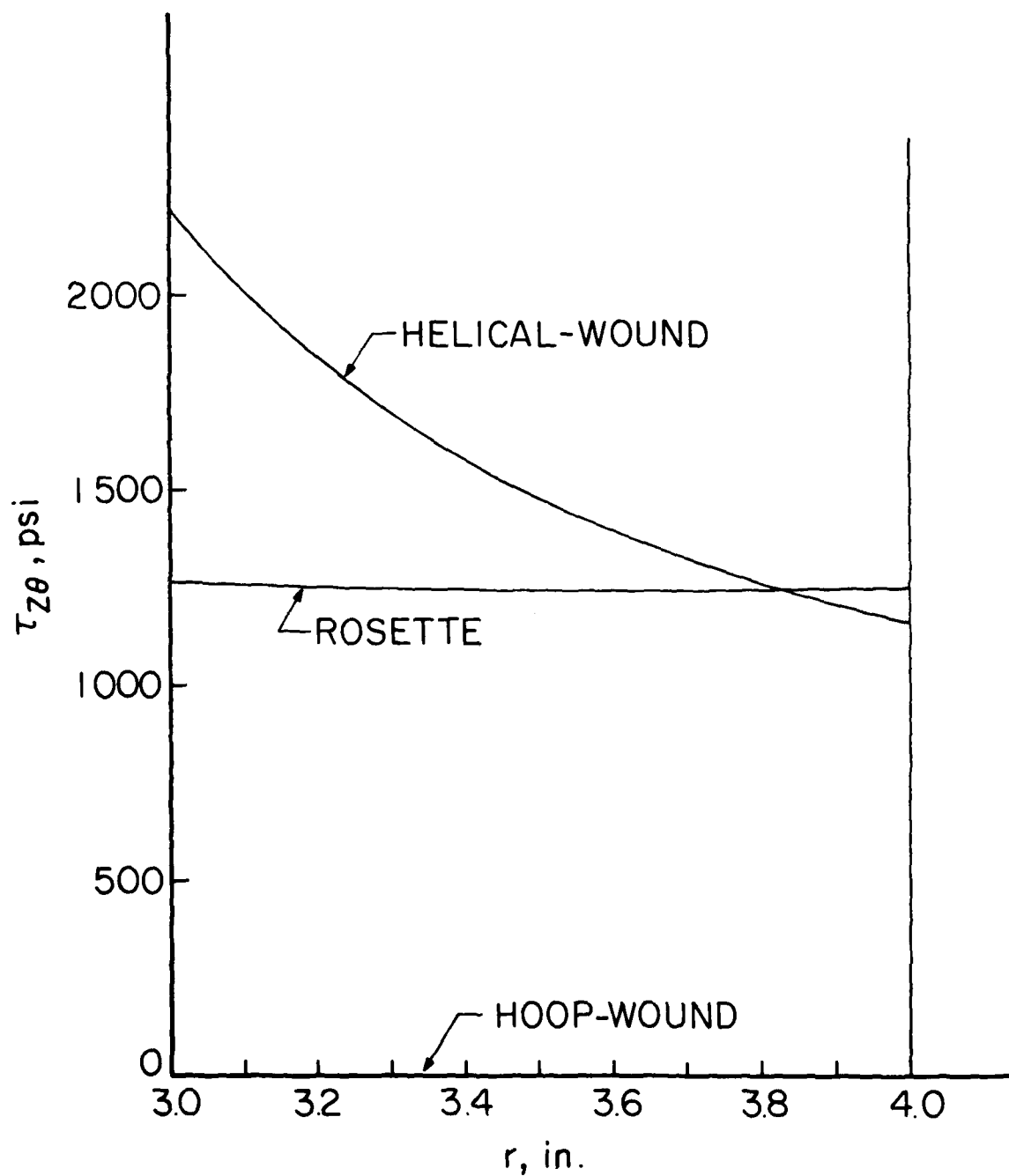


Figure 8. Shear Stress Distribution

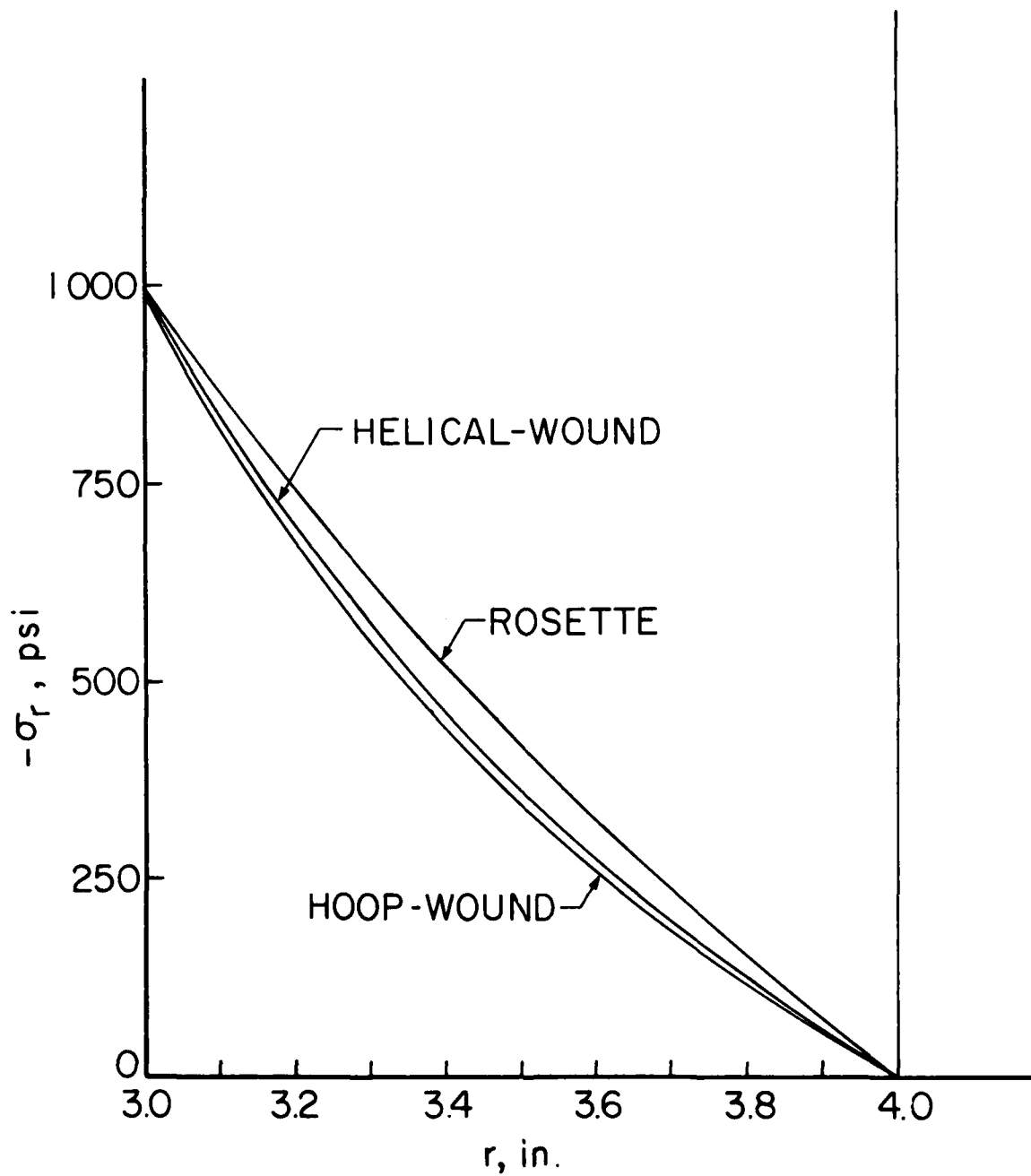


Figure 9. Radial Stress Distribution